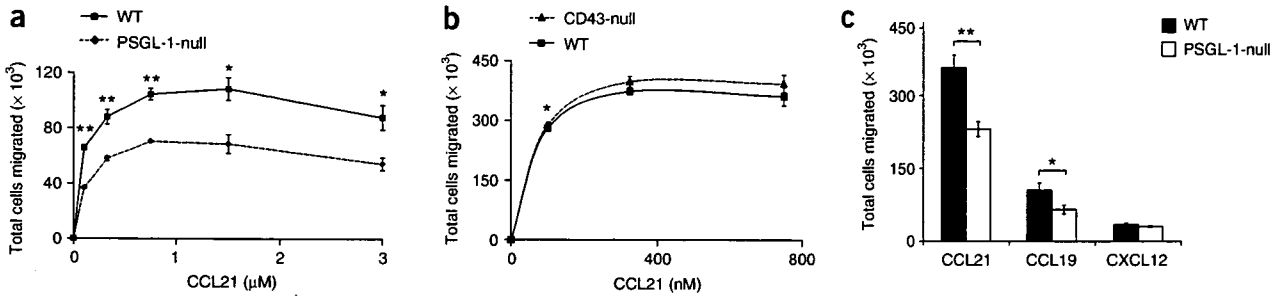

Figure 4 PSGL-1 is required for efficient chemotaxis to CCL21 and CCL19 but not to CXCL12. (**a**) Competitive *in vitro* chemotaxis assays of lymphocytes from C57BL/6 wild-type and GFP-transgenic PSGL-1-null mouse donors (**a**) or wild-type and CD43-null mice (**b**); cells were incubated for 1 h in transwells with varying concentrations of CCL21. *, $P < 0.05$, and **, $P < 0.001$ (Student's *t*-test): 100 nM, $P = 0.0000066$, 375 nM, $P = 0.000071$, 750 nM, $P = 0.00016$, 1.5 μM, $P = 0.0029$, and 3 μM, $P = 0.0042$ (**a**); 100 nM, $P = 0.02$, 375 nM, $P = 0.06$, and 750 nM, $P = 0.17$ (**b**). (**c**) *In vitro* chemotaxis assays of purified T lymphocytes from wild-type and GFP-transgenic PSGL-1-null donors; cells were incubated for 2–3 h in transwells with 200 nM CCL21, CCL19 or CXCL12. *, $P < 0.05$, and **, $P < 0.001$ (Student's *t*-test). Data are mean (± s.d.) number of cells recovered from the lower chamber, after subtraction of the number of cells migrating in absence of chemotactic agent ($n = 3$ (**a**,**b**) or 4 (**c**) transwell replicates per point), and are representative of at least three independent experiments.

of PSGL-1 was restricted to T cells of both the naive and central memory types, we used purified T cells to confirm the results obtained above with unfractionated lymphocytes. We also evaluated two additional chemokines, CCL19 and CXCL12, also known to be involved in lymphocyte homing[24,25], in the transwell chemotaxis assay. Wild-type and PSGL-1-null T cells migrated equally toward CXCL12 ($P = 0.11$), whereas the response to CCL19 was approximately 30% weaker for T cells lacking PSGL-1, as was the case for CCL21 ($P = 0.004$ and $P = 0.002$, respectively; **Fig. 4c**). Thus, PSGL-1 enhanced the chemotactic response of T cells to the two SLO chemokines CCL21 and CCL19 but not to CXCL12.

CCL21 binds T cells in a PSGL-1-dependent way

Our data indicated that binding of chemokine to PSGL-1 might be the underlying cause of the enhanced chemotactic responses of T cells. If so, CCL21 and possibly CCL19 would bind T cells not only by means of their cognate chemokine receptor CCR7 (ref. 26) and cell surface–expressed glycosaminoglycans, including heparan sulfate and chondroitin sulfate[27], but also by means of PSGL-1. To demonstrate a chemokine–PSGL-1 interaction, we immobilized decreasing amounts of CCL21 or control CXCL12 on nitrocellulose and 'probed' with a fusion protein of PSGL-1 and immunoglobulin G (IgG). With this approach, we found that PSGL-1 bound immobilized CCL21 but not CXCL12 (**Fig. 5a**). To directly assess the interaction of CCL21 with PSGL-1 expressed on lymphocytes, we synthesized mouse CCL21 biotinylated at the N terminus. Staining lymphocytes with this reagent showed that both $CD4^+$ and $CD8^+$ T cells bound CCL21 with a biphasic pattern. Notably, $CCL21^{hi}$ $CD4^+$ and $CD8^+$ T cells from wild-type mice bound considerably more CCL21 than the corresponding T cells from PSGL-1-null mice (**Fig. 5b**). In contrast, binding of CCL21 to B cells produced a relatively strong monophasic signal that was not affected by PSGL-1 expression; PSGL-1 expression was much lower on B cells than on T cells (**Supplementary Fig. 3** online). The '$CCL21^{dim}$' cells represent T cells that have internalized CCL21. The conditions we used for the CCL21 binding assay were similar to those used for chemotaxis assay and thus allowed chemokine internalization. We also

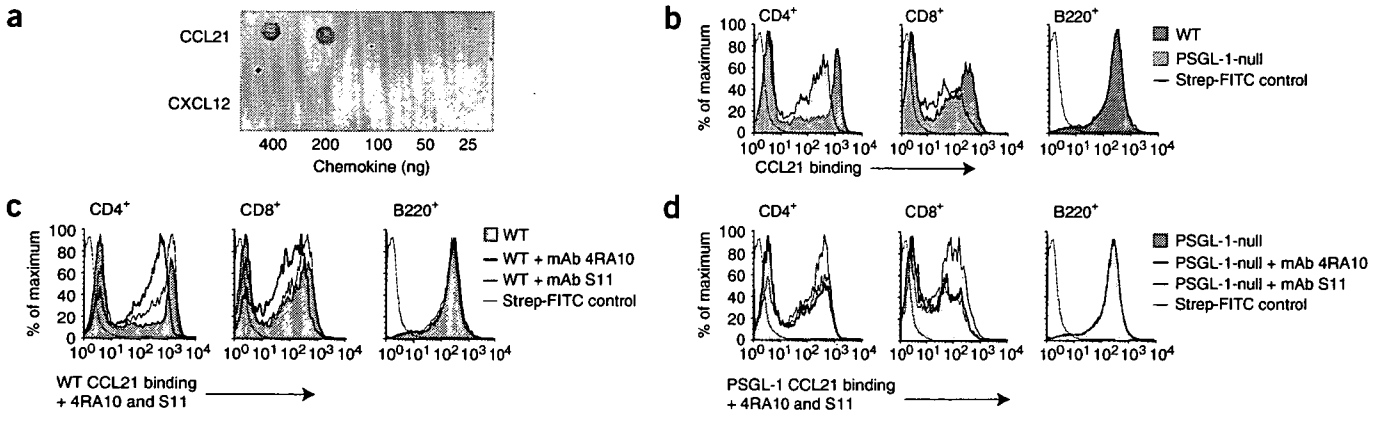

Figure 5 PSGL-1 binds CCL21. (**a**) Detection of CCL21 and CXCL12 immobilized on a nitrocellulose membrane with a PSGL-1–human IgG1 chimera and 'probed' with fluorescent anti–human IgG. (**b**) Flow cytometry of wild-type and PSGL-1-null lymphocytes incubated for 2 h with a mixture of biotin-CCL21 and fluorescein isothiocyanate–streptavidin (Strep-FITC), then co-stained with anti-CD4, anti-CD8 or anti-B220. (**c**,**d**) Flow cytometry of wild-type lymphocytes (**c**) and PSGL-1-null lymphocytes (**d**) incubated for 30 min with mAb 4RA10 (to PSGL-1) or mAb S11 (to CD43) before 2 h of incubation with fluorescein isothiocyanate–CCL21 followed by co-staining with anti-CD4, anti-CD8 or anti-B220. Fluorescein isothiocyanate–streptavidin staining without chemokine, negative control. Data are representative of four independent experiments.

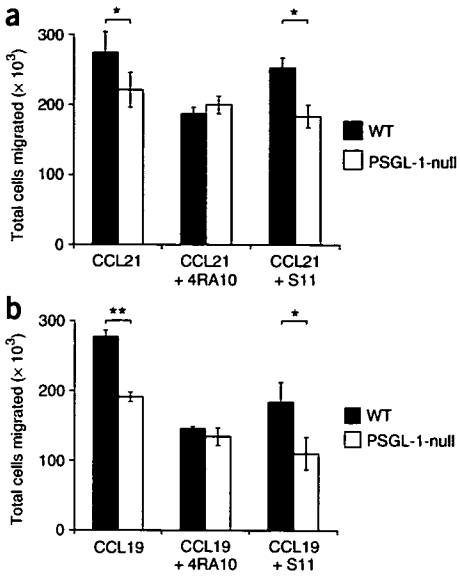

Figure 6 Chemotactic advantage of wild-type over PSGL-1-null T cells is blocked by mAb 4RA10 (to PSGL-1). Competitive *in vitro* transwell chemotaxis assay of the migration of C57BL/6 wild-type T cells and GFP-labeled PSGL-1-null T cells toward 200 nM CCL21 (**a**) or 200 nM CCL19 (**b**) after incubation of cells with mAb 4RA10 (to PSGL-1) or mAb S11 (to CD43). *, $P < 0.05$, and **, $P < 0.001$ (Student's *t*-test). Data are mean (± s.d.) number of cells recovered from the lower chamber after 2 h of incubation, after subtraction of the number of cells migrating in absence of chemotactic agent ($n = 4$ transwell replicates per point), and are representative of three independent experiments.

did CCL21 binding studies in the presence of sodium azide to prevent chemokine internalization. As expected, binding of CCL21 to T cells was monophasic in presence of sodium azide. However, although the difference in the binding of CCL21 to wild-type versus PSGL-1-null cells was still present, it was much less, as was the inhibition of CCL21 binding by antibody to PSGL-1 (anti-PSGL-1; **Supplementary Fig. 4** online).

The binding of mAb 4RA10 has been mapped to the N terminus of PSGL-1, a region also important for the binding of P-selectin and chemokines[22,28]. The binding of CCL21 to $CD4^+$ and $CD8^+$ T cells from wild-type mice was reduced with mAb 4RA10, such that it was similar to that of PSGL-1-null T cells (**Fig. 5c**), whereas the binding of CCL21 to B cells (**Fig. 5c**) or PSGL-1-deficient T cells (**Fig. 5d**) was not affected by mAb 4RA10. Pretreatment of cells with a mAb (S11) to CD43, another leukocyte mucin, had no effect on the CCL21 binding profiles. These results collectively demonstrated direct interaction of CCL21 with PSGL-1 expressed on $CD4^+$ and $CD8^+$ T cells.

Figure 7 Core 2 *O*-glycan branch formation on PSGL-1 causes loss of enhanced chemotaxis on activated T cells. (**a**) Competitive *in vitro* transwell chemotaxis assay of the migration of C57BL/6 wild-type and PSGL-1-null lymphocytes toward 200 nM CCL21, CXCL11 or CXCL9, 4 d after cells were activated with concanavalin A. (**b**) Chemotactic responses to 200 nM CCL21, of wild-type versus PSGL-1-null lymphocytes and of lymphocytes lacking C2GlcNAcT-I versus lymphocytes lacking both PSGL-1 and C2GlcNAcT-I, before activation (left; Lymph node cells) and 4 d after activation with concanavalin A (right; Activated T cells). *, $P < 0.05$, and **, $P < 0.001$ (Student's *t*-test; $n = 4$). Data are mean (± s.d.) number of cells recovered from the lower chamber after 2 h of incubation, after subtraction of the number of cells migrating in absence of chemotactic agent, and are representative of three independent experiments.

Anti-PSGL-1 blocks the PSGL-1-enhanced chemotaxis

The inhibition of the CCL21–PSGL-1 interaction by treatment with mAb 4RA10 suggested that this mAb might inhibit the chemotactic advantage associated with T cells expressing PSGL-1 and responding to CCL21 or CCL19. To test that hypothesis, we added neutralizing amounts of mAb 4RA10 to the competitive chemotaxis assay. This eliminated the chemotactic advantage of wild-type cells in response to both CCL21 and CCL19 ($P = 0.91$ and $P = 0.84$, respectively; **Fig. 6**). In contrast, PSGL-1-null cells remained at a chemotactic disadvantage (CCL21, $P = 0.02$; CCL19, $P = 0.01$) in the presence of mAb S11 (to CD43). Thus, mAb 4RA10 abrogated the PSGL-1-mediated chemotactic advantage, whereas mAb S11 did not.

PSGL-1-enhanced chemotaxis is lost on activated T cells

Activated T cells upregulate the chemokine receptor CXCR3 (ref. 29) and become responsive to the inflammatory chemokines CXCL9, CXCL10 and CXCL11 (also called Mig, IP-10 and I-TAC). Analysis of T cells activated by the mitogen concanavalin A showed that chemotactic migration of activated PSGL-1-null T cells toward CXCL9 and CXCL11 was not lower; indeed these cells showed a trend to migrate better than wild-type cells (20–40% increase over wild-type cells; $P = 0.06$ and $P = 0.31$, respectively; **Fig. 7a**). Activated T cells remained responsive to CCL21 (ref. 30) but migrated equivalently to this chemokine with or without PSGL-1 ($P = 0.30$; **Fig. 7a**), suggesting that the PSGL-1-enhanced migration to CCL21 and CCL19 does not apply to all differentiation states of T cells.

T cell activation results in the coordinated upregulation of several glycosyltransferases required for functional P-selectin ligand formation on PSGL-1 (ref. 17). Expression of core 2 *O*-glycan–branched sialyl Lewis X on Thr17 as well as sulfation of Tyr13 on the N terminus of mouse PSGL-1 are essential for the binding of P-selectin[31]. Loss of the CCL21–PSGL-1 effect on activated T cells could thus be due to upregulation of core 2–branched sialyl Lewis X on Thr17, which may block the putative CCL21 interaction with sulfated Tyr13 and/or sulfated Tyr15 on PSGL-1 (ref. 22). To test for such a function for core 2 *O*-glycans, we determined whether T cells lacking C2GlcNAcT-I maintained their PSGL-1-linked chemotactic advantage after activation. We therefore compared the chemotactic response of T cells deficient in C2GlcNAcT-I with that of T cells lacking both C2GlcNAcT-I and PSGL-1. Consistent with our short-term homing results, resting T cells from donors lacking both C2GlcNAcT-I and PSGL-1 were at a chemotactic disadvantage relative to those from

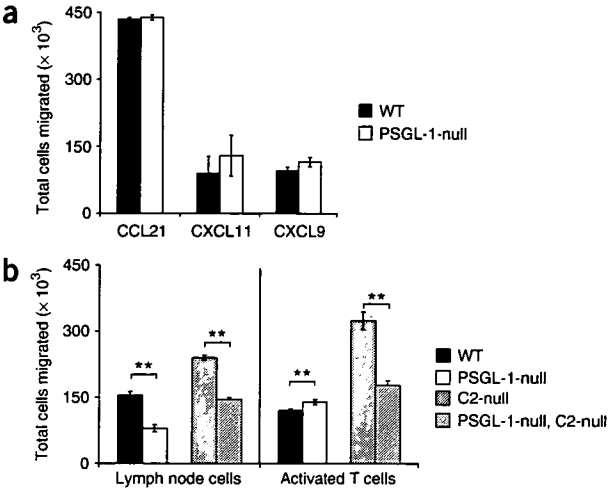

donors lacking only C2GlcNAcT-I ($P = 0.00000023$; **Fig. 7b**). However, contrary to our finding with activated C2GlcNAcT-I-sufficient T cells, activated C2GlcNAcT-I-null T cells maintained their advantage over activated T cells lacking both C2GlcNAcT-I and PSGL-1 ($P = 0.000013$; **Fig. 7b**); in fact, the activated C2GlcNAcT-I-null T cells migrated twofold better than activated T cells from either wild-type or PSGL-1-null donors. Thus, the core 2 *O*-glycan branch seemed to interfere with the postulated CCL21–PSGL-1 interaction.

DISCUSSION

Our data have demonstrated a previously unrecognized function of PSGL-1 in the homing of T cells to SLOs by enhancing chemotactic responses to the SLO chemokines CCL21 and CCL19. The effect of PSGL-1 on homing to SLOs was restricted to naive and central memory T cells and did not extend to B cells, which express less PSGL-1 and are much less dependent on CCL21 or CCL19 for homing to SLOs than are T cells[9]. The observed lower chemotactic response of PSGL-1-null T cells to CCL21 and CCL19 was not due to complete loss of chemotactic responsiveness of specific T cell subsets. Given that loss of PSGL-1 expression similarly affects the homing of all T cell subsets to SLOs, we propose that loss of PSGL-1 expression results in an overall lower migratory response of T cells.

PSGL-1, originally identified as a ligand for P-selectin, can bind all three selectins and has a central proadhesive function in many inflammatory settings[17]. The possibility of involvement of any of the selectins in the mechanism of action driving the enhanced homing of T cells to SLOs can be ruled out based on our competitive homing experiments using selectin-deficient recipients and/or C2GlcNAcT-I-null donor lymphocytes. Furthermore, resting T cells (naive and central memory T cells) do not have C2GlcNAcT activity and consequently do not express PSGL-1 capable of binding P-selectin and L-selectin.

The mechanism by which PSGL-1 functions in its chemotaxis-enhancing capacity is unclear at present. The findings of inhibition of *in vivo* lymphocyte homing by blockade with mAb 4RA10, inhibition of the binding of CCL21 to PSGL-1 by mAb 4RA10, and mAb 4RA10–mediated abrogation of the wild-type chemotactic advantage over PSGL-1-null T cells are consistent with a functional interaction between PSGL-1 and CCL21 or CCL19. It is likely that such an interaction would require the N-terminal tyrosine sulfates of mouse PSGL-1, as is the case for the binding of CCL27 to human PSGL-1 (ref. 22). The binding of CCL21 and/or CCL19 to PSGL-1 on the lymphocyte might precede the chemokine-CCR7 interaction on the same cell in a 'pass-on' process. The physiological utility of this CCL21–PSGL-1 or CCL19–PSGL-1 interaction may be to capture chemokine, thereby counteracting a rapid loss that might otherwise occur in the bloodstream during transfer from the apical surface of HEVs to the rolling lymphocyte. PSGL-1 is a highly extended mucin[32] localized on microvilli[33] and might be well adapted for rapid and efficient transfer of the chemokine between the interacting cells. Alternatively, the CCL21–PSGL-1 or CCL19–PSGL-1 interaction may induce signaling by means of PSGL-1 (refs. 34,35) and actively contribute to an enhanced chemotactic response.

The L-selectin required by naive T cells to enter SLOs is down-regulated once T cells become activated, thus preventing activated T cells from re-entering SLOs. Notably, analysis of transgenic mice expressing 'non-sheddable' L-selectin has indicated that in addition to shedding of L-selectin, a second mechanism might exist that prevents re-entry of activated T cells into SLOs, as activated T cells expressing 'non-sheddable' L-selectin migrate less efficiently into lymph nodes than the corresponding naive T cells[36]. The PSGL-1-enhanced chemotaxis described here could be the basis of such a second mechanism, as the effect was lost in a core 2 *O*-glycan–dependent way on activated T cells. T cell activation–induced upregulation of core 2 *O*-glycan–branched sialyl Lewis X on Thr17 located on the N terminus of PSGL-1 may thus serve a dual purpose: first, to support the formation of functional selectin ligands, enabling trafficking of these cells to sites of inflammation, and second, to limit responses to chemokines such as CCL21 and CCL19, which in concert with L-selectin shedding would prevent activated T cells from re-entering SLOs.

The implications of the absence of PSGL-1 and of compromised homing to SLOs on normal immune function are not apparent at present and need to be explored in PSGL-1-deficient animals. Analysis by the Consortium for Functional Glycomics has shown that immunoglobulin production is decreased in PSGL-1-deficient mice in response to immunization with the T cell–dependent antigen keyhole limpet hemocyanin (http://www.functionalglycomics.org/glycomics/publicdata/phenotyping.jsp).Whether this effect is due to reduced homing of T cells to SLOs, however, remains to be determined.

The functional interaction of PSGL-1 with homing chemokines shown here substantially expands the recognized functional scope of this molecule. Our findings may stimulate reconsideration of previous analyses using PSGL-1-null mice, soluble recombinant PSGL-1 or anti-PSGL-1, as such treatments may have influenced normal lymphocyte recirculation by a heretofore unappreciated mechanism. This newly identified function of PSGL-1 may extend to other examples of chemokine interactions and possibly to some cytokines as well. Indeed, there have been several reports indicating anti-inflammatory effects of recombinant soluble PSGL-1 or neutralizing mAb to PSGL-1 that could not be explained by selectin antagonism[37–39].

METHODS

Chemokines. All chemokines were chemically synthesized 'in-house' with tBoc (tertiary butyloxycarbonyl) solid-phase chemistry. Chemokines were purified by high-performance liquid chromatography, and mass was confirmed by electrospray mass spectrometry[40]. Biotinylated CCL21 was produced by the coupling of biotinamidohexanoic acid *N*-hydroxysuccinimide ester (Sigma) to the N terminus of CCL21 before the 'deprotection' and refolding steps.

Mice. C57BL/6, PSGL-1-deficient C57BL/6 and P-selectin-deficient C57BL/6 mice were from the Jackson Laboratory. CD-1 mice were from Charles River Laboratories. The generation of C2GlcNAcT-1-deficient mice[20], CD43-deficient mice[41], E-selectin-deficient mice[42] and mice expressing green fluorescent protein (GFP) ubiquitously from the cytomegalovirus-enhancer chicken actin hybrid promoter[43] has been described. Mice deficient in both GlcNAc6ST-1 and GlcNAc6ST-2, mice deficient in both C2GlcNAcT-1 and PSGL-1, and mice transgenic for GFP and deficient in PSGL-1 were generated by intercrossing mice of the appropriate specific genotypes[15,44]. All mice were backcrossed at least eight generations on a C57BL/6 background. Mice were maintained in specific pathogen–free conditions and all animal experiments were done according to institutional guidelines and were approved by the Animal Care Committee of the University of British Columbia and the Institutional Animal Care and Use Committee of the University of California San Francisco.

Preparation of Fab fragments. Fab fragments of mAb 4RA10 (ref. 37) and rat IgG1 (eBioscience) were generated and purified with the ImmunoPure Fab Preparation Kit following the manufacturer's recommendations (Pierce). Fragments were concentrated and washed into PBS on a Centricon-10 (Millipore). Protein purity was assessed by nonreducing SDS-PAGE, followed by detection with Coomassie blue (GelCode Blue; Pierce). Protein concentration was determined by measurement of the absorbance at 280 nm.

***In vivo* homing assays with mAb blockade.** Lymphocyte-homing assays were done as described[15]. Mesenteric node lymphocytes from 6- to 10-week-old CD-1 mice were isolated and were labeled with 5 μM CMFDA

(5-chloromethylfluorescein diacetate; Molecular Probes). Cells (3×10^7) were mixed with 100 μg of mAb 4RA10 or rat IgG1 (eBioscience) in 200 μl of PBS. Fab fragments (25 μg) of mAb 4RA10 or rat IgG1 were used for Fab inhibition experiments. The mixture was injected into the tail veins of age-matched (12-week-old) wild-type mice (C57BL/6) and mice doubly deficient in GlcNAc6ST-1 and GlcNAc6ST-2. At 1 h after injection, mice were killed and SLOs were collected. Lymphocytes in these organs were 'teased out' with two 25-gauge needles. The fractional content of $CMFDA^+$ cells in lymphocyte suspensions was determined by flow cytometry (FACScan; Becton-Dickinson). For each suspension, 5×10^5 cells were analyzed and acquired with CellQuest software (Becton-Dickinson). Data were normalized for each mouse by division of the fractional value of $CMFDA^+$ cells by the mean of the fractional values for all of the wild-type mice in the experiment.

Cell preparation for *in vivo* homing assays with knockout mice and competitive transwell chemotaxis assays. Superficial cervical, brachial, inguinal, mesenteric and axillary lymph nodes were removed from age-matched donor mice and were dissociated into single-cell suspensions with a stainless steel sieve in RPMI medium (Gibco) containing 10% (vol/vol) FBS, 2 mM L-glutamine and 50 μM 2-mercaptoethanol and were kept at 4 °C. In some experiments, samples were depleted of B cells with anti–mouse IgG Dynabeads (Invitrogen). In experiments requiring 'concanavalin A blasts', cells were cultured for 4 d in complete RPMI medium with 2% (vol/vol) interleukin 2–containing media, conditioned by myeloma X.653 cells transfected with cDNA encoding mouse IL-2, and 4 μg/ml of concanavalin A. When cells were ready for use, they were washed, and viable cells were counted on a hemocytometer. Non-GFP^+ lymph node cells were labeled for 5 min at 25 °C with 0.2 μM CFDA-SE (5-(and-6)-carboxyfluorescein diacetate succinimidyl ester; Molecular Probes) in RPMI medium containing 10% (vol/vol) FCS or for 8 min at 37 °C with 8 μM Cell Tracker Orange (CTO; Molecular Probes) in Hank's balanced-salt solution (14185-052; Invitrogen Life Technologies). Immediately after being labeled, cells were washed once with RPMI medium containing 10% (vol/vol) FBS, then once with Hank's balanced-salt solution (Gibco). A ratio of 1:1 was determined by the cell count on the hemocytometer, then was verified by flow cytometry before injection. Cells were combined based on flow cytometry data. A final cell count was obtained with beads as described[41].

***In vivo* homing assays with knockout mice.** After 2×10^6 cells of each dye-labeled sample were combined and suspended in Hank's balanced-salt solution, they were injected intravenously into wild-type C57BL/6, P-selectin-deficient or E-selectin-deficient recipient mice, which were killed 1 h later in the same order in which they were injected. Peripheral blood, spleens, Peyer's patches and brachial, inguinal, mesenteric and axillary lymph nodes were collected and kept on ice. Peripheral blood was collected by perfusion with 2.5 mM EDTA in PBS and was added to a solution containing 2.5 mM EDTA and 4% (vol/vol) FBS in PBS. All lymph nodes were pooled, as were Peyer's patches. Spleens, lymph nodes and Peyer's patches were mechanically dissociated into single-cell suspensions into RPMI medium containing 10% (vol/vol) FBS. Peripheral blood and spleens were treated for 10 and 5 min, respectively, with red blood cell–lysis buffer. All cells were washed and resuspended three times with media. Subsets were determined with mAb to CD8 (CL8938B; clone CT-CD8b; Cedarlane), mAb to CD4 (553730; clone GK1.5; BD Pharmingen), mAb to CD44 (17-0441; clone IM7; eBiosciences) and mAb to B220 (553091; clone RA3-6B2; BD Pharmingen). CFDA-SE was detected in the FL1 channel and CTO was detected in the FL2 channel of the FACScan (Becton Dickinson). Flow cytometry data were analyzed with FlowJo (TreeStar) and Excel (Microsoft) software and were normalized to the results of wild-type mice.

Competitive transwell chemotaxis assay. Chemotaxis buffer (600 μl; RPMI medium, 100 mM HEPES, pH 7.2, and 0.5% (wt/vol) BSA) containing chemokine was added to the lower chamber of a transwell plate (Costar), followed by prewarming for a minimum of 1 h at 37 °C. GFP- or dye-labeled cells were transferred to chemotaxis buffer prewarmed to 37 °C and were resuspended at a density of 10×10^6 viable cells per ml. Prepared mixed cells (100 μl) were added to the upper transwell chamber, followed by incubation for 2–3 at 37 °C. In antibody inhibition experiments, 50 μl antibody was added to the upper transwell chamber first, followed by 50 μl of mixed cells at a density of 20×10^6 viable cells per ml. Migrated cells were quantified by flow cytometry (FACScan, Becton-Dickinson) and cell-counting beads as described[41]. Flow cytometry data were analyzed with FlowJo and Excel software. Absolute cell counts were normalized for differences in starting numbers and were adjusted relative to 'no-chemokine' controls.

PSGL-1–human IgG1 chimera. The cDNA encoding the 45 N-terminal amino acids of mature mouse PSGL-1 (primers: mPSGL-1_fw_ClaI, 5′-CCATCGA TGGGCAGGTGGTTGGGGATGACG-3′; mPSGL-1_45_rv_EcoRI, 5′ CCGGA ATTCCGGCACGGTGGTTGGCAGCTC-3′) and cDNA encoding the human IgG1 hinge, CH2 and CH3 domains (primers: hIgG_fw_EcoRI, 5′-CCGGAAT TCCGGACATGCCCACCGTGCCCA-3′; hIgG_rv_BamHI, 5′-CGCGGATCC GCGTCAGAGGCTCTTCTGCGT-3′) was amplified by PCR. The template for the IgG1 tag was a vector encoding human IgG1 (ref. 45). PCR products were cloned into the respective cloning sites of a pBluescriptII SK cloning vector. The insert was then cloned into a pMXpie expression vector containing the leader sequence of mouse CD43 followed by a Flag tag[46] using *ClaI* and *NotI* restrictions sites, respectively. The vector was transiently transfected into Chinese hamster ovary cells with Lipofectamin Plus (Invitrogen). After 48 h, supernatants were purified on a protein G column.

For binding assays, 400 ng to 25 ng of CCL21 and CXCL12 was dotted onto Hybond ECL nitrocellulose membranes (Amersham Biosciences). Membranes were blocked for 2 h with 5% (wt/vol) BSA in Tris-buffered saline and were then incubated for 2 h with 50 μg/ml of PSGL-1–IgG. For detection of binding, membranes were incubated for 1 h with anti–human IgG (Jackson ImmunoResearch) and then were incubated for 1 h with Alexa Fluor 680–streptavidin (Molecular Probes). Membranes were analyzed with the Odyssey Infrared Imaging System (LI-COR).

Chemokine binding assays. Biotin-CCL21 (0.67 nmol) and 1.1 μg fluorescein isothiocyanate–streptavidin (BD Pharmingen) were mixed and were preincubated for 30 min in 30 μl chemotaxis buffer plus 2% (wt/vol) BSA, then were mixed with 1×10^6 lymphocytes in 70 μl chemotaxis buffer plus 0.5% (wt/vol) BSA, followed by incubation for 2 h at 37 °C. Cells were then washed once with 10% (vol/vol) FCS in PBS, and were stained for lymphocyte markers CD4, CD8 or B220. After 20 min of incubation, cells were washed twice in 10% (vol/vol) FCS in PBS and were analyzed with a FACSCalibur (Becton Dickinson).

Statistical analysis. Microsoft Excel was used for all statistical analyses. Statistical significance was determined by the two-tailed, unpaired Student's *t*-test; $\alpha = 0.05$ for all tests.

Note: Supplementary information is available on the Nature Immunology website.

ACKNOWLEDGMENTS

We thank R. Beavis for discussions; K.M. McNagny for critically reading the manuscript; P.D. Ziltener and M.J. Ford for technical assistance; J. Marth (University of California at San Diego) for C2GlcNAcT-1-deficient mice; D.C. Bullard (University of Alabama) for E-selectin-deficient mice; I. Weissman (Stanford University) for mice expressing GFP; G. McLean (University of Texas Health Sciences Center at Houston) for the vector encoding for human IgG1; and F. Melchers (Basel Institute of Immunology) for myeloma X.653 cells transfected with cDNA encoding mouse IL-2. Supported by the National Institutes of Health (R01GM57411 and R01GM23547 to S.D.R.), the Canadian Institutes for Health Research (J.S.M.; MOP-64267 and MOP-77552 to H.J.Z.) and Deutsche Forschungsgemeinschaft (S.N.)

AUTHOR CONTRIBUTIONS

J.S.M., H.J.Z. and K.U., S.D.R. independently discovered the PSGL-1 requirement for T cell homing; K.M.V. did the competitive homing assays; K.U. and M.S.S. did the mAb inhibition homing assays; M.J.W. designed and did the chemotaxis and CCL21 binding assays; S.N. contributed to the CCL21 binding studies; D.A.C. contributed to the experimental design of the competitive *in vivo* and *in vitro* studies; P.O. produced all chemokines; J.R.-N. provided anti-PSGL-1 and helped with the inhibition studies; H.J.Z. and S.D.R. supervised research and coordinated ongoing work; K.M.V. and H.J.Z. wrote the first draft of the manuscript; and all authors contributed to discussions and preparation of the manuscript.

COMPETING INTERESTS STATEMENT
The authors declare no competing financial interests.

Published online at http://www.nature.com/natureimmunology
Reprints and permissions information is available online at http://npg.nature.com/reprintsandpermissions

1. von Andrian, U.H. & Mempel, T.R. Homing and cellular traffic in lymph nodes. *Nat. Rev. Immunol.* **3**, 867–878 (2003).
2. Rosen, S.D. Ligands for L-selectin: homing, inflammation, and beyond. *Annu. Rev. Immunol.* **22**, 129–156 (2004).
3. Miyasaka, M. & Tanaka, T. Lymphocyte trafficking across high endothelial venules: dogmas and enigmas. *Nat. Rev. Immunol.* **4**, 360–370 (2004).
4. Forster, R. *et al.* CCR7 coordinates the primary immune response by establishing functional microenvironments in secondary lymphoid organs. *Cell* **99**, 23–33 (1999).
5. Gunn, M.D. *et al.* Mice lacking expression of secondary lymphoid organ chemokine have defects in lymphocyte homing and dendritic cell localization. *J. Exp. Med.* **189**, 451–460 (1999).
6. Weninger, W. & von Andrian, U.H. Chemokine regulation of naive T cell traffic in health and disease. *Semin. Immunol.* **15**, 257–270 (2003).
7. Campbell, J.J. & Butcher, E.C. Chemokines in tissue-specific and microenvironment-specific lymphocyte homing. *Curr. Opin. Immunol.* **12**, 336–341 (2000).
8. Lowe, J.B. Glycan-dependent leukocyte adhesion and recruitment in inflammation. *Curr. Opin. Cell Biol.* **15**, 531–538 (2003).
9. Okada, T. *et al.* Chemokine requirements for B cell entry to lymph nodes and Peyer's patches. *J. Exp. Med.* **196**, 65–75 (2002).
10. Tang, M.L., Steeber, D.A., Zhang, X.Q. & Tedder, T.F. Intrinsic differences in L-selectin expression levels affect T and B lymphocyte subset-specific recirculation pathways. *J. Immunol.* **160**, 5113–5121 (1998).
11. Gauguet, J.M., Rosen, S.D., Marth, J.D. & von Andrian, U.H. Core 2 branching β1,6-*N*-acetylglucosaminyltransferase and high endothelial cell *N*-acetylglucosamine-6-sulfotransferase exert differential control over B- and T-lymphocyte homing to peripheral lymph nodes. *Blood* **104**, 4104–4112 (2004).
12. Sackstein, R. The lymphocyte homing receptors: gatekeepers of the multistep paradigm. *Curr. Opin. Hematol.* **12**, 444–450 (2005).
13. Ley, K. The role of selectins in inflammation and disease. *Trends Mol. Med.* **9**, 263–268 (2003).
14. Rossi, F.M. *et al.* Recruitment of adult thymic progenitors is regulated by P-selectin and its ligand PSGL-1. *Nat. Immunol.* **6**, 626–634 (2005).
15. Uchimura, K. *et al.* A major class of L-selectin ligands is eliminated in mice deficient in two sulfotransferases expressed in high endothelial venules. *Nat. Immunol.* **6**, 1105–1113 (2005).
16. Kawashima, H. *et al. N*-acetylglucosamine-6-*O*-sulfotransferases 1 and 2 cooperatively control lymphocyte homing through L-selectin ligand biosynthesis in high endothelial venules. *Nat. Immunol.* **6**, 1096–1104 (2005).
17. Ley, K. & Kansas, G.S. Selectins in T-cell recruitment to non-lymphoid tissues and sites of inflammation. *Nat. Rev. Immunol.* **4**, 325–335 (2004).
18. Spertini, O., Cordey, A.S., Monai, N., Giuffre, L. & Schapira, M. P-selectin glycoprotein ligand 1 is a ligand for L-selectin on neutrophils, monocytes, and CD34+ hematopoietic progenitor cells. *J. Cell Biol.* **135**, 523–531 (1996).
19. Martinez, M. *et al.* Regulation of PSGL-1 interactions with L-selectin, P-selectin, and E-selectin: role of human fucosyltransferase-IV and -VII. *J. Biol. Chem.* **280**, 5378–5390 (2005).
20. Ellies, L.G. *et al.* Core 2 oligosaccharide biosynthesis distinguishes between selectin ligands essential for leukocyte homing and inflammation. *Immunity* **9**, 881–890 (1998).
21. Pilkington, K.R., Clark-Lewis, I. & McColl, S.R. Inhibition of generation of cytotoxic T lymphocyte activity by a CCL19/macrophage inflammatory protein (MIP)-3β antagonist. *J. Biol. Chem.* **279**, 40276–40282 (2004).
22. Hirata, T. *et al.* Human P-selectin glycoprotein ligand-1 (PSGL-1) interacts with the skin-associated chemokine CCL27 via sulfated tyrosines at the PSGL-1 amino terminus. *J. Biol. Chem.* **279**, 51775–51782 (2004).
23. Fukuda, M. Leukosialin, a major O-glycan-containing sialoglycoprotein defining leukocyte differentiation and malignancy. *Glycobiology* **1**, 347–356 (1991).
24. Baekkevold, E.S. *et al.* The CCR7 ligand elc (CCL19) is transcytosed in high endothelial venules and mediates T cell recruitment. *J. Exp. Med.* **193**, 1105–1112 (2001).
25. Scimone, M.L. *et al.* CXCL12 mediates CCR7-independent homing of central memory cells, but not naive T cells, in peripheral lymph nodes. *J. Exp. Med.* **199**, 1113–1120 (2004).
26. Yoshida, R. *et al.* Secondary lymphoid-tissue chemokine is a functional ligand for the CC chemokine receptor CCR7. *J. Biol. Chem.* **273**, 7118–7122 (1998).
27. Hirose, J., Kawashima, H., Yoshie, O., Tashiro, K. & Miyasaka, M. Versican interacts with chemokines and modulates cellular responses. *J. Biol. Chem.* **276**, 5228–5234 (2001).
28. Frenette, P.S. *et al.* P-Selectin glycoprotein ligand 1 (PSGL-1) is expressed on platelets and can mediate platelet-endothelial interactions *in vivo*. *J. Exp. Med.* **191**, 1413–1422 (2000).
29. Loetscher, M. *et al.* Chemokine receptor specific for IP10 and mig: structure, function, and expression in activated T-lymphocytes. *J. Exp. Med.* **184**, 963–969 (1996).
30. Willimann, K. *et al.* The chemokine SLC is expressed in T cell areas of lymph nodes and mucosal lymphoid tissues and attracts activated T cells via CCR7. *Eur. J. Immunol.* **28**, 2025–2034 (1998).
31. Xia, L. *et al.* N-terminal residues in murine P-selectin glycoprotein ligand-1 required for binding to murine P-selectin. *Blood* **101**, 552–559 (2003).
32. Li, F. *et al.* Visualization of P-selectin glycoprotein ligand-1 as a highly extended molecule and mapping of protein epitopes for monoclonal antibodies. *J. Biol. Chem.* **271**, 6342–6348 (1996).
33. Moore, K.L. *et al.* P-selectin glycoprotein ligand-1 mediates rolling of human neutrophils on P-selectin. *J. Cell Biol.* **128**, 661–671 (1995).
34. Hidari, K.I., Weyrich, A.S., Zimmerman, G.A. & McEver, R.P. Engagement of P-selectin glycoprotein ligand-1 enhances tyrosine phosphorylation and activates mitogen-activated protein kinases in human neutrophils. *J. Biol. Chem.* **272**, 28750–28756 (1997).
35. Ba, X., Chen, C., Gao, Y. & Zeng, X. Signaling function of PSGL-1 in neutrophil: tyrosine-phosphorylation-dependent and c-Abl-involved alteration in the F-actin-based cytoskeleton. *J. Cell. Biochem.* **94**, 365–373 (2005).
36. Galkina, E. *et al.* L-selectin shedding does not regulate constitutive T cell trafficking but controls the migration pathways of antigen-activated T lymphocytes. *J. Exp. Med.* **198**, 1323–1335 (2003).
37. Rivera-Nieves, J. *et al.* Critical role of endothelial P-selectin glycoprotein ligand 1 in chronic murine ileitis. *J. Exp. Med.* **203**, 907–917 (2006).
38. Hicks, A.E., Nolan, S.L., Ridger, V.C., Hellewell, P.G. & Norman, K.E. Recombinant P-selectin glycoprotein ligand-1 directly inhibits leukocyte rolling by all 3 selectins *in vivo*: complete inhibition of rolling is not required for anti-inflammatory effect. *Blood* **101**, 3249–3256 (2003).
39. Sumariwalla, P.F., Malfait, A.M. & Feldmann, M. P-selectin glycoprotein ligand 1 therapy ameliorates established collagen-induced arthritis in DBA/1 mice partly through the suppression of tumour necrosis factor. *Clin. Exp. Immunol.* **136**, 67–75 (2004).
40. Clark-Lewis, I., Mattioli, I., Gong, J.H. & Loetscher, P. Structure-function relationship between the human chemokine receptor CXCR3 and its ligands. *J. Biol. Chem.* **278**, 289–295 (2003).
41. Carlow, D.A., Corbel, S.Y. & Ziltener, H.J. Absence of CD43 fails to alter T cell development and responsiveness. *J. Immunol.* **166**, 256–261 (2001).
42. Bullard, D.C. *et al.* Infectious susceptibility and severe deficiency of leukocyte rolling and recruitment in E-selectin and P-selectin double mutant mice. *J. Exp. Med.* **183**, 2329–2336 (1996).
43. Corbel, S.Y. *et al.* Contribution of hematopoietic stem cells to skeletal muscle. *Nat. Med.* **9**, 1528–1532 (2003).
44. Merzaban, J.S., Zuccolo, J., Corbel, S.Y., Williams, M.J. & Ziltener, H.J. An alternate core 2 β1,6-*N*-acetylglucosaminyltransferase selectively contributes to P-selectin ligand formation in activated CD8 T cells. *J. Immunol.* **174**, 4051–4059 (2005).
45. McLean, G.R., Nakouzi, A., Casadevall, A. & Green, N.S. Human and murine immunoglobulin expression vector cassettes. *Mol. Immunol.* **37**, 837–845 (2000).
46. Drew, E., Merzaban, J.S., Seo, W., Ziltener, H.J. & McNagny, K.M. CD34 and CD43 inhibit mast cell adhesion and are required for optimal mast cell reconstitution. *Immunity* **22**, 43–57 (2005).